Plant Physiology Preview. Published on June 21, 2019, as DOI:10.1104/pp.19.00231

Short Title: Role of DSP4 in snRNA maturation and pollen growth

Authors for correspondence:
Yunfeng Liu +86-18275823130 yunfengliu_bio@126.com
Bin Yu +01-4024722125 byu3@unl.edu.

Title:
DSP1 and DSP4 act synergistically in snRNA 3' end maturation and pollen growth

Xuepiao Pu[1, *], Chunmei Meng[2,*], Weili Wang[1,*], Siyu Yang[1], Yuan Chen[3], Qingjun Xie[4], Bin Yu[5, §], Yunfeng Liu[1, §]

[1] State Key Laboratory for Conservation and Utilization of Subtropical Agro-bioresources, College of Life Science and Technology, Guangxi University, 100 Daxue Road, Nanning, Guangxi 530004, China
[2] Life Sciences Institute, Guangxi Medical University, Nanning, 530021, China
[3] Plant Gene Expression Center, USDA-ARS and Dept. of Plant and Microbial Biology, UC-Berkeley, Albany, CA 94710, USA
[4] State Key Laboratory for Conservation and Utilization of Subtropical Agro-Bioresources, Guangdong Provincial Key Laboratory of Plant Molecular Breeding, South China Agricultural University, Guangzhou, 510642 China
[5] Center for Plant Science Innovation and School of Biological Sciences, University of Nebraska, Lincoln, NE 68588–0660, USA

* These authors contributed equally to this work.
§ Corresponding authors.

One-sentence summary:

DSP1 and DSP4 function synergistically in pollen development, and promote pre-snRNA transcription and 3' end processing efficiency and accuracy.

Authors' contributions

Y.L. and B.Y. designed the study and wrote the manuscript; X.P. and Y.L. performed most of the experiments; S. Y. made vectors construction; C.M. performed super thin sections of the anthers; Y.C. collected pollen sample from plants; W.W. performed statistical analysis about pollen development; Q.X. analyzed protein cellular localization.

Abstract:

Small nuclear RNAs (snRNAs) play essential roles in spliceosome assembly and splicing. Most snRNAs are transcribed by the DNA-dependent RNA polymerase II (Pol II) and require 3' end endonucleolytic cleavage. We have previously shown that the Arabidopsis (*Arabidopsis thaliana*) Defective in snRNA Processing 1 (DSP1) complex, composed of at least five subunits, is responsible for snRNA 3' maturation and is essential for plant development. Yet, it remains unclear how DSP1 complex subunits act together to process snRNAs. Here we show that DSP4, a member of the metallo-β-lactamase family, physically interacts with DSP1 through its β-Casp domain. Null *dsp4-1* mutants have pleiotropic developmental defects, including impaired pollen development, and reduced pre-snRNA transcription and 3' maturation, resembling the phenotype of the *dsp1-1* mutant. Interestingly, *dsp1-1 dsp4-1* double mutants exhibit complete male sterility and reduced pre-snRNA transcription and 3' end maturation, unlike *dsp1-1* or *dsp4-1*. In addition, Pol II occupancy at snRNA loci is lower in *dsp1-1 dsp4-1* than in either single mutant. We also detected miscleaved pre-snRNAs in *dsp1-1 dsp4-1,* but not in *dsp1-1* or *dsp4-1*. Taken together, these data reveal that DSP1 and DSP4 function is essential for pollen development, and that the two cooperatively promote pre-snRNA transcription and 3' end processing efficiency and accuracy.

Key words: snRNA transcription and 3' maturation, *DSP1*, *DSP4*, pollen, Arabidopsis.

Introduction

Small nuclear RNAs (snRNAs) (Hadjiolov et al., 1966), a class of non-coding RNAs, are the basal components of the spliceosome, and play essential roles in pre-mRNA splicing (Black et al., 1985; Ray et al., 1997; Guo et al., 2009). Their biogenesis involves transcription and subsequent processing steps. In Arabidopsis (*Arabidopsis thaliana*), the DNA-dependent RNA polymerase II (Pol II) synthesizes the primary snRNA transcripts (pre-snRNAs) U1, U2, U4, U5, and U12, but not U6, which is transcribed by the RNA polymerase III (Pol III) (Carbon et al., 1987, Vankan & Filipowicz, 1988). Following transcription, pre-snRNAs are subjected to endonucleolytic cleavage at specific sites to remove the RNA fragment transcribed beyond the 3' end of mature snRNAs.

In metazoans, snRNA 3' end maturation requires the Integrator Complex (INT) (Baillat et al., 2005). INT contains at least fourteen subunits (Baillat et al., 2005; Chen and Wagner, 2010), associates with the C-terminal domain (CTD) of the largest subunit of Pol II, and depends on transcription for complex formation. It co-transcriptionally cleaves pre-snRNAs upstream of the required 3'box RNA motif (Uguen and Murphy, 2003, 2004; Baillat et al., 2005; Chen and Wagner, 2010). Integrator Subunit 11 (INT11) is a putative member of the metallo-β-lactamase/ β-CASP family of RNA endonucleases, is homologous to the cleavage and polyadenylation specificity factor 73 kDa (CPSF73) that catalyzes pre-mRNA 3' end cleavage, and is considered to be the enzyme that cleaves pre-snRNAs at the 3' end. INT9 is also a CPSF73 homolog, but lacks key amino residues critical for endonuclease activity (Baillat et al., 2005; Li et al., 2016). INT9 and INT11 form a heterodimer through their C-terminal domains and this interaction is critical for the 3' end processing efficiency of

pre-snRNAs (Albrecht & Wagner, 2012; Wu et al., 2017). Besides snRNA 3' maturation, INT also functions in other biological processes, including transcription termination of mRNAs, maturation of some viral-derived miRNAs, prevention of viral infection, biogenesis of enhancer RNAs, and dynein localization at the nuclear envelope (Jodoin et al., 2013; Gardini et al., 2014; Stadelmayer et al., 2014; Lai et al., 2015; Skaar et al., 2015; Xie et al., 2015; Li et al., 2016). Consistent with the importance of these functions, mutations in INT subunits often result in embryo lethality (Hata and Nakayama, 2007; Rutkowski & Warren, 2009; Ezzeddine et al., 2011; Kapp et al., 2013).

Plant snRNA 3' maturation does not depend on transcription, although it requires a 3' box motif, whose sequence differs from its metazoan counterpart (Connelly & Filipowicz, 1993). In plants, the Defective in snRNA Processing 1 (DSP1) complex and the CPSF complex, both of which contain CPSF73-I, are responsible for the 3' end cleavage of pre-snRNAs and pre-mRNAs, respectively. The DSP1 complex is composed of at least four additional subunits, DSP1 to DSP4 (Liu et al., 2016). Disruption of DSP1, DSP3, DSP4, or CPSF73-I, but not DSP2, impairs pre-snRNA processing, resulting in increased accumulation of pre-snRNAs. However, like in *int* mutants, the accumulation of mature snRNAs is not altered in the *dsp* mutants. Interestingly, Pol II occupancy and transcription of pre-snRNAs are reduced in *dsp1*, suggesting that DSP1 may also promote snRNA transcription. Supporting this, DSP1 was shown to bind snRNA gene promoters. Furthermore, all available null *dsp1-2, dsp2-1, dsp3-2*, and *cpsf73-1* mutants are embryonically lethal, while *dsp1* and *cpsf73-I* have defective pollen development (Xu et al., 2006; Liu et al., 2016). These observations suggest

102 that the DSP1 complex plays multiple important roles in development.

103

104 While DSP4 has sequence similarities with INT9, but it does not interact with CPSF73-I, a
105 homolog of INT11 (Liu et al., 2016). Until now, no null *DSP4* mutant allele has been
106 analyzed, and the function of DSP4 in pre-snRNA 3' maturation and development is still not
107 understood. Here, we show that an amorphic *dsp4-1* mutation impairs growth and male
108 fertility, and reduces pre-snRNA transcription and 3' end processing in Arabidopsis. These
109 phenotypes resembled those of *dsp1*. Interestingly, *dsp1-1 dsp4-1* double mutants are
110 completely male sterile. Pre-snRNA 3' end processing and transcription is further reduced in
111 *dsp1-1 dsp4-1* relative to *dsp1-1* or *dsp4-1*. Moreover, the cleavage accuracy of pre-snRNA 3'
112 end is reduced in *dsp1 dsp4* when compared with wild type or single mutants. These results,
113 together with the fact that DSP4 interacts with the ARM domain of DSP1 through its β-Casp
114 domain, demonstrate that DSP4 and DSP1 cooperatively promote snRNA transcription and 3'
115 maturation, and regulate pollen and plant development.

116

117

Results

The *dsp4-1* mutation impairs development and male gametophyte transmission.

We previously showed that knockdown of *DSP4* with artificial miRNAs causes developmental defects. To further evaluate the function of *DSP4*, we obtained a *dsp4-1* allele (*SALK_005904*) that contains a T-DNA insertion in the 10th intron of *DSP4* (Supplemental Fig. S1A). Reverse transcription quantitative PCR (RT-qPCR) analysis using specific primers that span the 10th intron revealed that the *DSP4* transcript levels in *dsp4-1* were greatly reduced relative to Col (wild type; WT). Moreover, the size of the *DSP4* transcript was longer in *dsp4-1* than that in Col (Supplemental Fig. S1B). Sequencing analysis showed that the increased size of the *DSP1* transcript was caused by retention of the 11th intron that led to a premature stop codon (Supplemental Fig. S1C). Like *DSP4* knockdown lines, *dsp4-1* had delayed growth and fertility; several aborted seeds were detected in *dsp4-1* siliques (Fig. 1A, B). To demonstrate that *dsp4-1* is responsible for the observed phenotypes, a wild-type copy of the *DSP4* genomic DNA, fused with a *GFP* reporter gene driven by its native promoter (*pDSP4::DSP4-GFP*), was transformed into *dsp4-1*. Expression of the wild-type *DSP4* rescued the developmental defects of *dsp4-1*.

The ratio of heterozygous versus WT plants in the progeny of *DSP4/dsp4-1* crosses was 1.24:1 which is less than the 2:1 ratio expected by Mendelian inheritance (Supplemental Table S1). This result suggested that, like for *DSP1* (Liu et al., 2016), *DSP4* may also reduce gametophyte transmission. To determine whether *dsp4-1* affects female or male gametophyte

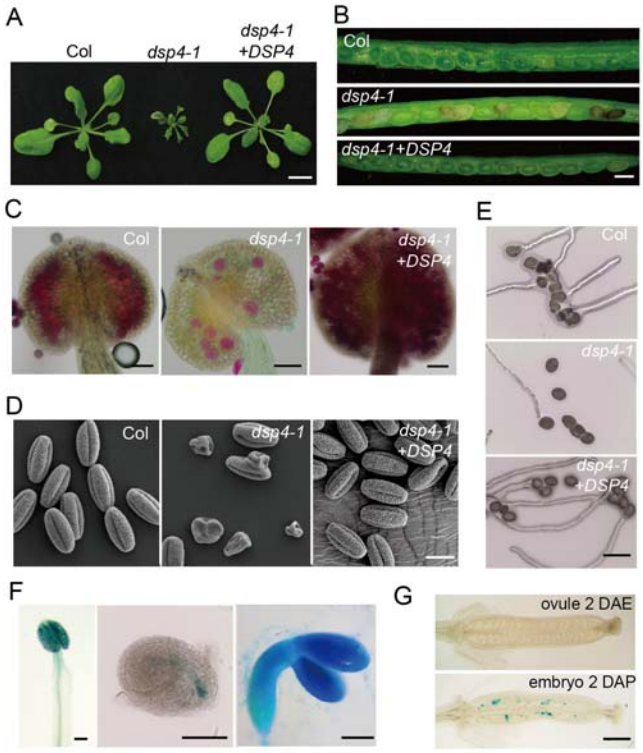

Figure 1. *dsp4-1* causes pleiotropic developmental defects.
(A) 25-day-old plants with 9 resette-leaves of Col, *dsp4-1*, and *dsp4-1* harboring the *pDSP4::DSP4-GFP* transgene. (B) Developing seeds in siliques of various genotypes. (C) Alexander staining of pollen grains in anthers of various genotypes. (D) Pollen structures of various genotypes detected by scanning electron microscopy (SEM). (E) *In vitro* germination of pollen of various genotypes. Images were obtained at 8 h after incubation in BK medium. (F) Histochemical GUS staining of pollen (left), embryo sac (middle), and embryos (right) of plants containing the *pDSP4::GUS* transgene. (G) Histochemical staining of GUS in the siliques of plants containing the *pDSP4::GUS* transgene. DAE: days after emasculation; DAP: days after pollination. (E) and (G) show a representative image of one out of five plants analyzed. Scale bars = 5 mm (A), 1 mm (B), 30 μm (C), 10 μm (D), 20 μm (E), 0.1 mm (F), 0.5 mm (G).

transmission, we performed reciprocal crosses between *DSP4*/*dsp4-1* and WT. When *DSP4/dsp4-1* was used as a pollen donor, the gametophyte penetration of *dsp4-1* was distorted (Supplemental Table S2). In contrast, when *DSP4/dsp4-1* was used as the female parent, *dps4-1* transmitted normally, suggesting that male, but not female, gametophyte transmission was impaired. To verify the influence of *DSP4* on pollen development, we

145 examined pollen viability using Alexander staining (Chen et al., 2016). There was only a
146 small number of purple-stained (viable) pollen in *dsp4-1* anthers, suggesting that most grains
147 were sterile (Fig. 1C). Furthermore, scanning electron microscopy (SEM) analysis showed
148 that more than half of the pollen grains of *dsp4-1* were shrunken and irregular in shape (Fig.
149 1D) compared with those of WT. Consistently, most *dsp4-1* pollen grains failed to germinate
150 *in vitro* (Fig. 1E). The *pDSP4::DSP4-GFP* transgene was able to rescue pollen structure,
151 viability, and germination in *dsp4-1* (Fig. 1C, D, E), demonstrating that *DSP4* is required for
152 pollen development.

153 Next, we examined if the expression pattern of *DSP4* is consistent with its function in pollen
154 development. We generated a transgenic plant expressing a GUS reporter gene under the
155 control of the *DSP4* promoter. Histochemical staining showed that GUS was weakly
156 expressed in leaves and roots, but not in stems, emerging flowers, and unfertilized ovules and
157 eggs (Fig. 1G; Supplemental Fig. S1D). High GUS expression was detected in pollen (Fig.
158 1F), in agreement with a role for DSP4 in pollen development. GUS was also detected in
159 fertilized eggs and developing embryos (Fig. 1F), suggesting that DSP4 may have an
160 additional role in embryo development. Indeed, we found that aborted *dsp4-1* seeds contained
161 embryos arrested at the globular stage (Supplemental Fig. S1E).
162

163 **DSP4 interacts with the ARM domain of DSP1 via its β-Casp domain**

164 As DSP4 interacts with DSP1, and is required for snRNA 3' end maturation and development,
165 it is possible that it participates in snRNA processing and development as a component of the
166 DSP1 complex. To evaluate this possibility, we first examined if DSP4 localized in the

167 nucleus, where snRNA 3' end processing occurs. We analyzed GFP localization in *dsp4-1*
168 plants harboring the *pDSP4::DSP4-GFP* transgene and found that, indeed, the signals were
169 enriched in the nucleus of pollen and embryo cells (Supplemental Fig. S2A, B, C).
170
171 Next, we sought to further confirm and characterize the physical interaction between DSP4
172 and DSP1 by determining the putative protein domains that mediate the interaction. DSP4 is
173 a homolog of CPSF73, but is catalytically inactive. It contains an MBL-fold
174 metallo-hydrolase domain (aa 101-280), a β-Casp (metallo-β-lactamase-associated CPSF-73
175 Artemis SNM1/PSO2; aa 374-478) domain, and a c-terminal region. Targeting these three
176 domains, we generated three truncated DSP4 proteins, DSP4-tr1 (amino acids (aa) 1-348),
177 DSP4-tr2 (aa 333-485), and DSP4-tr3 (aa 483-699) (Fig. 2A). DSP1 contains three clusters of
178 Armadillo/beta-catenin-like repeats (ARM, ~ 40 aa for each repeat), which provide
179 solvent-accessible surfaces for binding of other substrates. We constructed three truncated
180 versions of DSP1, DSP1-tr1 (aa 1-230), DSP1-tr2 (aa 224-504), and DSP1-tr3 (aa 498-1133),
181 to cover these three ARM clusters (Fig. 2B). We first examined the interaction of truncated
182 DSP1 proteins with truncated DSP4 proteins using bimolecular fluorescence
183 complementation (BiFC). The co-expression of DSP1-tr2-cYFP and DSP4-tr2-nYFP, but no
184 other pairs of truncated proteins (Fig. 2C), resulted in YFP fluorescence signals, suggesting
185 that the second ARM domain of DSP1 and the β-Casp domain of DSP4 are responsible for
186 the DSP1-DSP4 interaction. We next used co-immunoprecipitation (co-IP) to confirm this
187 possibility. We co-expressed, in *Nicotiana benthamiana*, three truncated DSP4 proteins fused
188 with a MYC tag at their C-terminus, with DSP1-tr2-GFP, or three GFP-fused truncated DSP1

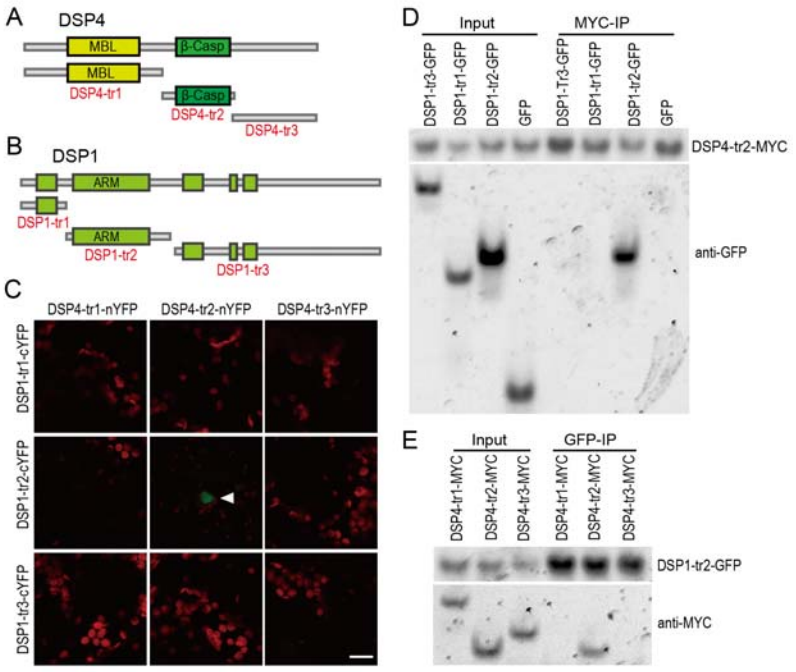

Figure 2. The β-Casp domain of DSP4 and the second ARM cluster of DSP1 mediate the DSP1-DSP4 interaction.
(A) and (B) Schemes of full-length and truncated DSP4 (A) and DSP1 (B) used for testing the DSP1-DSP4 interaction. (C) The interactions of various forms of DSP4 with truncated DSP1 was detected by bimolecular fluorescence complementation (BiFC) in *N. benthamiana* epidermal cells. Paired DSP1-trs-cYFP and DSP4-trs-nYFP fusion proteins were infiltrated into *N. benthamiana* leaves. Green: BiFC signal (originally YFP fluorescence). Red: autofluorescence of chlorophyll. Scale bars=10 μm. (D) Co-immunoprecipitation (Co-IP) of DSP4-tr2 with truncated DSP1 proteins. (E) Co-IP of DSP1-tr2 with truncated DSP4 truncation proteins. IP was performed using antibodies recognizing MYC (D) or GFP (E). After IP, truncated DSP4-MYC and DSP1-GFP were detected by western blot using antibodies against MYC and GFP, respectively. Input: total protein before IP.

proteins with DSP4-tr2-MYC. After IP, we could detect DSP1-tr2-GFP in DSP4-tr2-MYC and DSP4-tr2-MYC in the DSP1-tr2-GFP precipitates (Fig. 2D, E), demonstrating that the β-Casp domain of DSP4 and the ARM cluster 2 of DSP1 are essential and sufficient to mediate the DSP1-DSP4 interaction.

dsp1-1 dsp4-1 **double mutants have severe developmental defects**

195 The interaction of DSP4 with DSP1 raised the possibility that they function as part of a
196 complex in pre-snRNA 3' maturation and development. To test this, we examined the genetic
197 interaction between *dsp1-1* and *dsp4-1*. We constructed a *dsp1-1 dsp4-1* double mutant by
198 crossing the two single mutants. We were able to identify *dsp1-1 dsp4-1* plants in the F2
199 population, but with an extremely low ratio of penetration (2/300), which indicates an
200 impaired male and/or female gametophyte transmission. To test this hypothesis, we made
201 reciprocal crosses of *dsp1-1/dsp1-1 DSP4/dsp4-1* or *DSP1/dsp1-1 dsp4-1/ dsp4-1* with WT.
202 The transmission rate of the double mutations was dramatically reduced relative to single
203 mutations when the double mutants were used as pollen donors (Supplemental Table S3). In
204 contrast, this double mutation had a nearly normal penetration rate when WT was used as
205 pollen donor. These results suggest that *dsp1-1 dsp4-1* further reduced male gametophyte
206 transmission rate relative to the single mutations.

207 Compared with *dsp1-1* or *dsp4-1*, *dsp1-1 dsp4-1* had increased sterility, a strong reduction in
208 size, and an increase in crimped leaves (Fig. 3A, B). Double mutants also produced almost no
209 viable pollen, as seen by the lack of purple Alexander staining in anthers (Fig. 3C). The
210 grains produced were shrunken, irregular, and adhered together (Fig. 3D; Supplemental Fig.
211 S3A, E, F). Moreover, they failed to germinate *in vitro* (Supplemental Fig. S3B, F) and *in*
212 *vivo* (Fig. 3E; Supplemental Fig. S3G), revealing that *dsp1-1 dsp4-1* failed to produce
213 functional male gametes. These results demonstrate that *DSP1* and *DSP4* act additively in
214 development and pollen growth. To identify the stage of pollen development affected in
215 *dsp1-1 dsp4-1*, we examined pollen morphology in anthers, using transmission electron
216 microscopy (TEM). The male gametophytic microspores were divided into 14 developmental

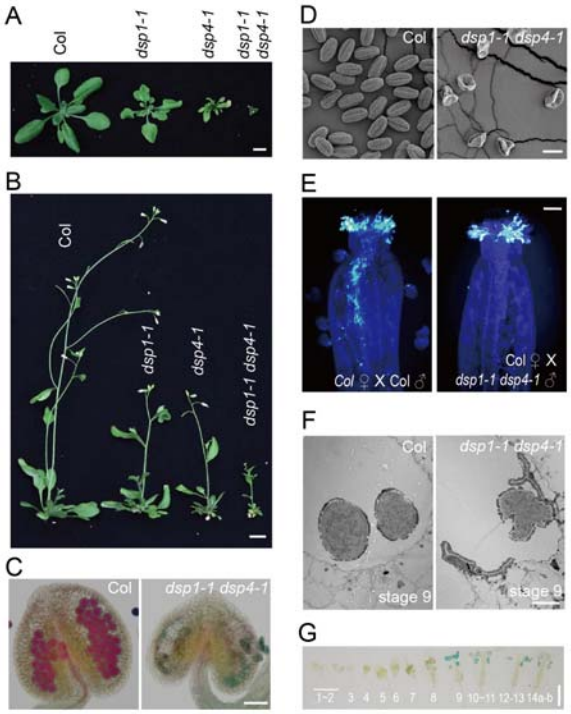

Figure 3. Morphological phenotypes of different genotype plants.
(A) and (B) 28-day-old (A) and 48-day-old (B) plants of Col, *dsp1-1*, *dsp4-1*, and *dsp1-1 dsp4-1*. Scale bars = 1.5 cm (A), 3 cm (B). (C) Alexander staining of pollen grains in anthers of Col and *dsp1-1 dsp4-1*. (D) Pollen structures of Col and *dsp1-1 dsp4-1* detected by SEM. (E) *In vivo* pollen germination of Col and *dsp1-1 dsp4-1*. Images were obtained 8 h after fertilization using *dsp1-1 dsp4-1* (right) or Col as a pollen donor (left). (F) Transmission electron micrographs showing the microspore structures of Col and *dsp1-1 dsp4-1* at anther stage 9. (G) Histochemical GUS staining of inflorescences from *pDSP4::GUS* transgenic plants at different developmental stages. Numbers in the image indicate the developmental stage of flowers. Scale bars = 30 μm (C), 10 μm (D), 0.5 mm (E), 10 μm (F) and 2 mm (G).

stages according to the typical pattern of dicotyledonous plants (Sanders et al., 1999). We collected anthers from WT and double mutant plants at parallel stages, then examined the ultrastructure of male microspores. No significant morphological structure difference was observed before stage 7 between WT and *dsp1-1 dsp4-1* anthers (Supplemental Fig. S3C). After stage 8, a large percentage of microspores became vacuolated and then degraded in *dsp1-1 dsp4-1* (Supplemental Fig. S3D). After stage 9, the microspores were completely or

223 partially devoid of cytoplasmic content (Fig. 3F). These results reveal that DSP1 and DSP4
224 may function after developmental stage 7 of microspores. Consistent with this result, the
225 expression of *DSP4* appeared in the male gametophyte at late stages (stage 9 to final stage)
226 (Fig. 3G), after meiosis, when haploid microspores were generated (Goldberg et al., 1993).
227
228 **DSP1 and DSP4 synergistically affect the accumulation of pre-snRNAs and snRNAs**
229 Next we examined if DSP1 and DSP4 cooperatively function in snRNA 3' end maturation.
230 We first tested the accumulation of various pre-snRNAs, including U1a, U2.3, U4.2, and
231 U5-6 in single and double mutants. As expected, the levels of all pre-snRNAs generated from
232 various snRNA loci were uniformly increased in *dsp1-1* and *dsp4-1*, relative to WT.
233 Furthermore, all pre-snRNAs were dramatically increased in *dsp1-1 dsp4-1* compared with
234 single mutants (Fig. 4A). A ribonuclease protection assay further confirmed this result (Fig.
235 4C, D), indicating that DSP1 and DSP4 may synergistically affect pre-snRNA processing.
236 We also examined the effect of DSP1 and DSP4 on the various mature snRNAs. Neither
237 *dsp1-1* nor *dsp4-1* altered the abundance of mature snRNAs (Fig. 4B, E), consistent with
238 observations in other *dsp* mutants and in *int* metazoan mutants (Tao et al., 2005; Liu et al.,
239 2016). Interestingly, both RT-qPCR and northern blot analyses showed that the levels of
240 mature snRNAs were reduced in *dsp1-1 dsp4-1* compared with WT and single mutants (Fig.
241 4B, E). The introduction of DSP4 without the β-Casp domain (*pDSP4::DSP4ΔCasp*) into the
242 *dsp4-1* mutant failed to rescue the phenotypes or pre-snRNA level, thus providing evidence
243 for the importance of the DSP4-DSP1 interaction in snRNA maturation (Supplemental Fig.
244 S4).

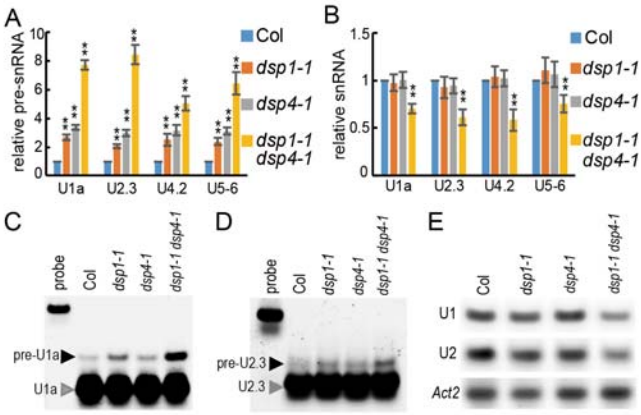

Figure 4. DSP1 and DSP4 synergistically promote snRNA 3' end maturation. (A) and (B) Accumulation of pre-snRNAs (A) and mature snRNA (B) in various genotypes detected by RT-qPCR. The pre-snRNA or mature snRNA levels were normalized to those of *ACT2* and compared with Col (Value set as 1). Values are means of three technical replicates. Bars indicate standard derivation (SD), * $P < 0.05$, ** $P < 0.01$ (t-test). Three biological replicates gave similar results. (C) and (D) Accumulation of pre-*U1a* and -*U2.3* RNAs in various genotypes detected by the RNase protection assay (RPA). Five micrograms of total RNA were incubated with U1a or U2.3 RNA probe. Black arrow indicates pre-snRNAs. Grey arrow indicates mature snRNAs. (E) Abundance of mature *U1* and *U2* snRNAs in various genotypes detected by northern blotting. *Act2* was blotted as the loading control.

DSP1 and DSP4 synergistically act in 3' end cleavage of pre-snRNAs

The increased accumulation of pre-snRNAs and the reduced abundance of snRNAs in *dsp1-1 dsp4-1* relative to single mutants suggest that DSP1 and DSP4 additively affect 3' end cleavage of pre-snRNAs. To test this possibility, we examined the effect of *dsp1-1 dsp4-1* on *in vitro* 3' end cleavage of *pre-U2.3* snRNA. The [P^{32}] labeled *pre-U2.3* snRNA, with a *poly-G* tail that prevents 3' end trimming, was incubated with nuclear protein extracts from inflorescences of Col, *dsp1-1*, *dsp4-1*, and *dsp1-1 dsp4-1* plants. After a 60-min reaction, RNAs were purified and resolved on a PAGE gel to examine the production of mature snRNAs. As previously reported, the amount of U2 RNAs was reduced in *dsp1-1* and *dsp4-1* compared with WT. Relative to *dsp1-1* or *dsp4-1,* the level of U2 was further reduced in

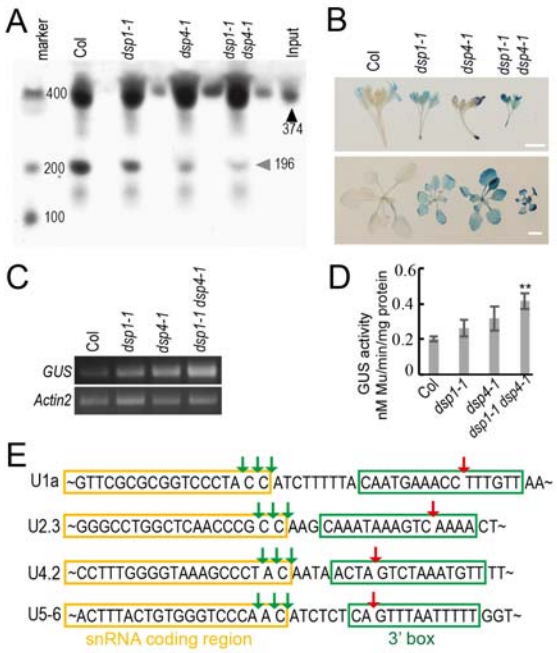

Figure 5. DSP1 and DSP4 cooperatively promote pre-snRNA 3' end cleavage. (A) *In vitro* 3' end processing of *pre-U2.3-polyG* in nuclear protein extracts of various genotypes. *In vitro* transcribed RNAs were labeled at 5'end, and incubated with the nuclear protein. Black arrow indicates the *pre-U2.3-polyG* input. Grey arrow indicates mature snRNA. (B) Histochemical staining of GUS in seedlings (bottom) and inflorescences (top) of Col, *dsp1-1, dsp4-1*, and *dsp1-1 dsp4-1* containing the *pU2::pre-U2-GUS* transgene. Scale bars = 4 mm (top), 1 cm (bottom). (C) *GUS* transcript levels determined by RT-PCR. *Actin 2* was amplified as a control. (D) *In vitro* GUS activities of protein inflorescence extracts from various genotypes. Protein extracts were quantified and incubated with 4-methylumbelliferyl β-D-glucuronide (4-MUG) and the reaction stopped by adding Na2CO3 after 10 min. The 4-methylumbelliferone (4-MU) products were measured with a spectrophotometer at 595 nm. Values are means of three technical replicates. Bars indicate standard derivation (SD), ** $P < 0.01$ (t-test). (E) 3' end cleavage site of pre-snRNAs in *dsp1-1 dsp4-1*. Green arrows indicate correct cleavage sites. Red arrows indicate improper cleavage sites.

256 *dps1-1 dsp4-1* (Fig. 5A), suggesting a cooperative effect of DSP1 and DSP4 on pre-snRNA

257 3' end processing.

258

259 Next, we used an *in vivo* GUS reporter system to validate the synergistic effect of DSP4 and

260 DSP1 on pre-snRNA processing. In this system, a GUS reporter gene was inserted

downstream of the 3' box within the pre-U2 gene containing the promoter, the coding region, and the 3' box (*pU2::pre-U2-GUS)*. This system has been used to monitor the effect of *dsp1-1* on pre-snRNA 3' cleavage efficiency, because GUS protein levels are inversely proportional to the cleavage upstream of the 3' box within pre-U2-GUS (Liu et al., 2016). We crossed three independent stable transgenic WT lines harboring *pU2::pre-U2-GUS* with *dsp1-1*, *dsp4-1*, and *dsp1-1 dsp4-1*, parallelly, and monitored GUS expression in these four genotypes. As expected, GUS levels were increased in *dsp1-1 and dsp4-1* relative to WT due to impaired 3' end maturation of *pre-snRNAs* (Fig. 5B), with three biological replicates giving similar results. We also observed that GUS expression levels and GUS activity were further increased in *dsp1-1 dsp4*-1 compared with single mutants (Fig. 5C, D). These results demonstrate that DSP4 is essential, and acts cooperatively with DSP1, in pre-snRNA 3' end cleavage.

We further examined the cleavage sites of mature snRNAs. Total RNA was attached with RNA adaptors, then reverse transcribed to single DNA strands. The randomly selected snRNAs from the U1, U2, U4, and U5 gene families were cloned using nested primers, then sequenced to examine the cleavage sites. In WT, *dsp1-1*, and *dsp4-1*, cleavage occurred upstream of the 3' box (Table 1). However, in *dsp1-1 dsp4-1*, a portion of snRNAs (6%~10%) was miscleaved at the 3' box (Table 1 and Fig. 5E). This result reveals that the accurate 3' cleavage of pre-snRNA requires the cooperative action of DSP1 and DSP4.

DSP4 impairs the occupancy of Pol II and DSP1 on snRNA loci

We have shown that *dsp1-1* affects the occupancy of Pol II in the promoter and coding regions of snRNAs but not in the 3' box. Since DSP4 acts synergistically with DSP1, we investigated if DSP4 and DSP1 also cooperatively influences Pol II occupancy at various regions of pre-snRNAs, using chromatin immunoprecipitation (ChIP) assay with antibodies recognizing RPB2, the second largest subunit of Pol II. We also included the downstream region (DS) of the 3′ box in the experiment because it has been shown that impaired snRNA 3' maturation can lead to pre-snRNA 3' end extension (Fukudome et al., 2017). Like *dsp1-1*, *dsp4-1* also reduced Pol II occupancy at the promoters and coding regions of *U1a* and *U2.3*, but not at the 3' box and DS regions (Fig. 6A). In contrast, Pol II had comparable occupancy levels at the *Actin2* loci in plants of all genotypes, or was not associated with the *Pol II C1* loci, which is an intergenic DNA region (Supplemental Fig. S5). These results suggest that, like DSP1, DSP4 is required for proper occupancy of Pol II at snRNA loci. Compared with single mutants, *dsp1-1 dsp4-1* further reduced the association of Pol II with the promoters and coding regions of U1a and U2.3. A higher occupancy of Pol II at the 3' box and the DS region was also observed in *dsp1-1 dsp4-1* relative to other genotypes. These data suggest that DSP1 and DSP4 may synergistically impact Pol II accumulation at snRNA genes.

The reduced Pol II occupancy at the promoter and coding regions of snRNAs in single or double mutants indicates that DSP1 and DSP4 may also positively regulate snRNA transcription. To test this possibility, we monitored pre-U2 transcription using a *pU2::pre-U2m-GUS* transgene. Since the *pre-U2m-GUS* RNA contains a mutated 3' box and cannot be cleaved there, its transcript levels or GUS levels in transgenic plants will not be

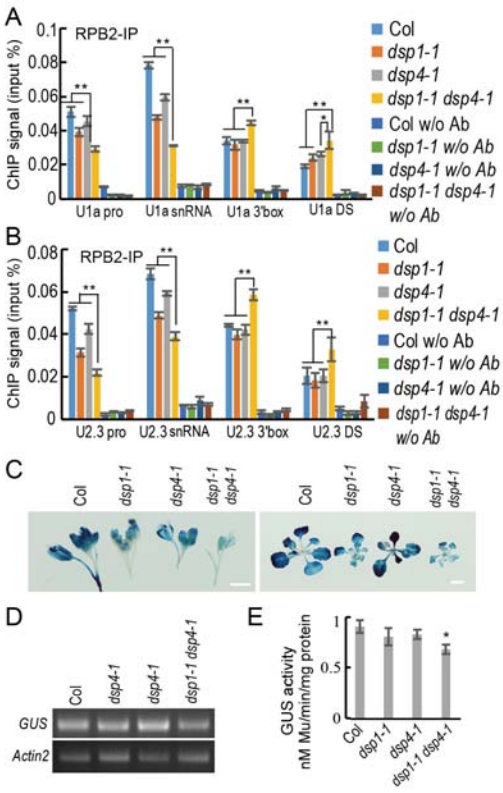

Figure 6. DSP1 and DSP4 synergistically promote pre-snRNA transcription. (A) and (B) Occupancy of Pol II at various sites of the *U1a* (A) and *U2.3* (B) snRNA loci in Col, *dsp1-1, dsp4-1*, and *dsp1-1 dsp4-1* detected by chromatin immunoprecipitation. pro: promoter; DS: down-stream region of snRNAs. Values are means of three technical replicates. Bars indicate standard derivation (SD), * $P < 0.05$, ** $P < 0.01$ (t-test). (C) GUS histochemical staining of 28-day-old seedlings (left) and 48-day-old inflorescences (right) in Col, *dsp1-1, dsp4-1,* and *dsp1-1 dsp4-1*, containing the *pU2::pre-U2m-GUS* transgene. *m*: mutated 3' box. Scale bars = 4mm (left), 1cm (right). (D) *GUS* transcript levels determined by RT-PCR. *Actin 2* was amplified as a control. (E) *In vitro* GUS activity in inflorescence protein extracts from various genotypes. The quantified total protein extracts were incubated with 4-MUG, the reaction stoped at 10 min, and 4-MU measured using spectrophotometer. Values are means of three technical replicates. Bars indicate standard derivation (SD), * $P < 0.05$ (t-test).

affected by 3' cleavage, and thus, it can be used to monitor pre-snRNA expression. We transformed this transgene into WT, crossed three independent stable transgenic lines into *dsp1-1*, *dsp4-1*, and *dsp1-1 dsp4-1*, parallelly, and examined the expression levels of GUS and *pre-U2m-GUS* in lines with the *pre-U2m-GUS* transgene, in all genotypes. GUS staining, RT-qPCR, and GUS activity analyses revealed elevated levels of *pre-U2m-GUS* in *dsp1-1,*

310 *dsp4-1*, and *dsp1-1 dsp4-1* compared with WT (Fig. 6C, D, E), with three biological
311 replicates giving similar results. In addition, the levels of pre-U2m-GUS were lower in
312 *dsp1-1 dsp4-1* than those of *dsp1-1* or *dsp4-1*. These data are consistent with the ChIP results
313 and show that DSP1 and DSP4 additively promote snRNA transcription.

314

315

316 **Discussion**

317 We have previously shown that the DSP1 complex is responsible for snRNA 3' maturation
318 (Liu et al., 2016). However, the precise roles of DSP components in this process, and how
319 these proteins coordinately catalyze snRNA 3' maturation, remained unknown. In this study,
320 we showed that DSP4 is an essential component of the DSP complex, evidenced by the
321 reduced pre-snRNA processing efficiency in *dsp4-1*. Moreover, DSP4 promotes snRNA
322 transcription, given its positive impact on Pol II occupancy at the promoters of snRNAs and
323 accumulation of pre-snRNAs. Our results also demonstrated that DSP1 and DSP4
324 synergistically influence CPSF73-I activity in snRNA 3' end cleavage, given the reduced
325 pre-snRNA cleavage efficiency and accuracy in *dsp1 dsp4* double mutants relative to *dsp1* or
326 *dsp4*.

327

328 What is the function of DSP4 in pre-snRNA 3' end cleavage? It has been known that CPSF73
329 and its homolog CPSF100 form a heterodimer, which is required for the endonuclease
330 activity that cleaves pre-mRNA during the polyadenylation process (Kolev et al., 2008;
331 Sullivan et al., 2009). Like CPSF100, DSP4 is a catalytically-inactive endonuclease of the
332 metallo-β-lactamase/β-CASP family. By analogy, DSP4 could act with CPSF73-I to form a
333 functional endonuclease for pre-snRNA 3' end cleavage. However, DSP4 does not interact
334 with CPSF73-I. Instead, DSP4 interacts with DSP1, which also interacts with CPSF73-I.
335 Moreover, these three proteins co-exist in a complex (Liu et al., 2016). These results raise the
336 possibility that DSP1 mediates the association between DSP4 and CSPF73-I, which in turn
337 facilitates CPSF73-I activity. This model predicts that DSP1 acts as a scaffold for the

assembly of an active endonuclease for pre-snRNA cleavage. Supporting this model, the DSP1 homolog in metazoans, INT4, interacts with and stabilizes the INT9-INT11 heterodimer, which is required for efficient pre-snRNA cleavage (Albrecht et al., 2018). Based on this model, we expected that *dsp1 dsp4* would have an impact on snRNA processing similar to *dsp1* or *dsp4*. However, we observed a synergistic effect of DSP1 and DSP4 on pre-snRNA processing activity. In addition, we found that the cleavage accuracy of pre-snRNAs by CPSF73-I is impaired in *dsp1 dsp4*. These results suggest that DSP1 and/or DSP4 have additional roles in regulating CPSF73-I cleavage efficiency and in defining cleavage sites for CPSF73-I. In metazoans, INT does not promote snRNA transcription, but in plants DSP1 and DSP4 appear to have cooperative roles in recruiting Pol II to the promoters of snRNA genes. These results suggest that the mechanisms promoting snRNA transcription differ between plants and metazoans, despite the common need for the snRNA activating protein complex (SNAPc) (Guiro & Murphy, 2017).

DSP4 also plays important roles in development. Interestingly, we find that DSP4 is highly expressed in pollen but not in ovules. In agreement, DSP4 is required for male germline development. However, the levels of mature snRNAs in *dsp4* are comparable with those in WT, suggesting that DSP4 has functions other than in snRNA biogenesis. DSP1 and DSP4 appear to have a synergistic effect on general and male germline development, given increased severity of phenotypes in *dsp1 dsp4* relative to single mutants. Although it is possible that the enhanced developmental defects of *dsp1 dsp4* are due to reduced snRNA levels, other possibilities exist. Both *DSP1* and *DSP4* mutations affect male gametophyte

development, while *srd2*, a mutant with defective snRNA transcription, was affected exclusively in the female gametophyte (Ohtani et al., 2008). This opposite phenotype also supports that DSP1 and DSP4 act on snRNA maturation and germline development through parallel pathways. It is possible that DSP1 and DSP4 have cooperative effects on the metabolism of other RNAs than snRNAs. Indeed, INT could affect transcription termination of some mRNAs and the biogenesis of enhancer RNAs in metazoans (Gardini et al., 2014; Stadelmayer et al., 2014; Lai et al., 2015; Skaar et al., 2015). Moreover, 3' extended transcription of snRNAs can produceprotein-coding transcripts from downstream snRNA loci (Fukudome et al., 2017). It is tempting to speculate that impaired 3' end cleavage in *dsp1 dps4* results in extended transcription of snRNAs and biogenesis of protein-coding transcripts, which may disrupt normal development.

Materials and Methods

Plant Materials

All T-DNA insertion mutants (*dsp4-1* SALK_005904; *dsp1-1* SALK_036641) were obtained from the Arabidopsis Biological Resources Center (https://abrc.osu.edu). All mutants are in the Columbia (Col) genetic background.

Plasmid Construction

The 1.97 kb promoter region of *DSP4* was cloned into *pENTR™/SD/D-TOPO* and subsequently cloned into *pGWB433* (Nakagawa et al., 2007) to generate the *pDSP4::GUS*

382 vector. The genomic fragments of *DSP4* containing the promoter and coding regions were
383 PCR amplified and cloned into *pGWB4* to generate the *pDSP4::DSP4-GFP* vector. The
384 truncated gene sequences of *DSP1* and *DSP4* were cloned into *pGWB4* and *pGWB17* to
385 generate *DSP1-trs-GFP and DSP4-trs-MYC* vectors, respectively. The primers used for
386 plasmid construction are listed in Supplemental Table S4.
387
388 **Histochemical GUS Staining**
389 For GUS staining, seedlings, inflorescence, or embryos dissected from immature seeds were
390 directly incubated overnight in the GUS staining buffer, in the dark and at 37℃. After
391 removing the chlorophyll in 70% (v/v) ethanol, GUS staining was observed under an
392 Olympus light microscope.
393
394 **Pollen Viability and Pollen Growth Assays**
395 Alexander staining was used to examine pollen viability as previously described (Xu et al.,
396 2015). *In vitro* pollen growth and *in vivo* pollen germination assays were performed as
397 described before (Chen et al., 2016). Briefly, for the *in vitro* pollen growth assay, mature
398 anthers were collected and vortexed in Brewbaker and Kwack (BK) lipid medium. Then, the
399 deposited pollen was spread on BK medium for 8 h, and observed by microscopy.
400
401 **Observation of pollen grain structures**
402 Ultrastructures of Pollen grain were examined according to Wang et al., (2017). Briefly**,**
403 anthers at various developmental stages were fixed, dehydrated, embedded in resin

(Epon812), and cut to semi-fine sections (0.6~0.8μm) with a Leica microtome for optical analyses. Serial sections were stained with toluidine blue. The slides were observed on an Olympus BX51 microscope. To observe the ultrastructure, the same blocks used for the optical microscope observations were cut to ~80 nm section with a diamond knife. The sections were collected on grids and sequentially stained with uranyl acetate and lead citrate. Following contrast and washing, the super-thin sections were observed by transmission electronic microscopy (JEOL, Japan).

U2.3 pre-snRNA *in vitro* processing assay

In vitro processing assays of *pre-U2.3-polyG* were performed as described before (Uguen & Murphy, 2003; Liu et al., 2016a). Briefly, *pre-snRNA-polyG* was generated by *in vitro* transcription using the T7 RNA Polymerase. RNA substrates were purified using an 8% polyacrylamide gel with 8 M urea, then 5' labeled with [P^{32}] using T4 Polynucleotide Kinase (T4 PNK). Then, the *pre-snRNA-polyG* RNA was incubated for 60 min with 2 μg nuclear proteins extracted from various plants, in a reaction buffer containing 10 mM HEPES pH 7.9, 50 mM KCl, 10% (v/v) glycerol, 20 mM creatine phosphate, 3 mM MnCl2, 3% (w/v) PEG, 1 mM DTT. Following the reaction, RNAs were extracted, purified, and resolved on 5% PAGE gels with 8 M urea. Radioactive signals were detected with a PhosphorImager.

Ribonuclease Protection Assay

Synthesized antisense RNA was labeled with [P^{32}] using T4 PNK. Five micrograms of total RNA extracted from inflorescences, using the Trizol Reagent, were incubated with

426 radiolabeled RNA probes. Ribonuclease protection assays were performed using RNase T1
427 and RNase A as previously described (Carey et al., 2013). After the reactions, the final
428 protected RNAs were separated in a 6% PAGE gel containing 8 M urea. Radioactive signals
429 were detected with a PhosphorImager.
430
431 **Pre-snRNA cleavage site analysis**
432 3' end cleavage sites of pre-snRNAs were analyzed according to Liu et al., (2016). Briefly,
433 RNA samples were dephosphorylated, and then ligated to a 3' RNA adaptor. The ligation
434 products were further purified with phenol/chloroform, ethanol precipitated, and then used as
435 templates for reverse transcription (primer sequences are in Supplemental Table S4). The RT
436 products were used as templates for nest-PCR amplification. The resulting PCR products
437 were cloned into *pGEM®-T Easy* Vector for sequencing.
438
439 **ChIP assay**
440 ChIP assays with anti-Pol II were performed as described before (Liu et al., 2016).
441 Anti-RPB2 (Abcam) antibodies were used for immunoprecipitation. Enrichment of the target
442 DNA loci relative to input were measured by quantitative PCR (qPCR) with three biological
443 replicates. The primers used in ChIP-PCR are listed in Supplemental Table S4.
444
445 **BiFC and Co-IP assay**
446 *DSP4* and *DSP1* fragments were fused at their N-termini with nYFP (*pEarleyGate201-YN*)
447 and cYFP (*pEarleyGate202-YC*), respectively. GV3101 *Agrobacterium* cells transformed

448 with different combinations of *DSP1-trs a*nd *DSP4-trs* were infiltrated into the leaves of
449 *Nicotiana benthamiana*. Epidermal cells were examined with confocal microscopy (Leica
450 TCS SP5). For the co-immunoprecipitation assay, a mixture of *Agrobacterium* containing
451 different combinations of DSP1-trs-GFP and DSP4-trs-MYC were expressed in N.
452 *benthamiana* leaves, and then used for immunoprecipitation assays as described before
453 (Zhang et al., 2013). The immunoprecipitated proteins were analyzed by western blotting.
454

455 **Statistical analyses**

456 The statistical analyses including Student's t-test were performed by Excel 2010 software.
457 The qPCR for each sample was replicated three times unless noted otherwise, the average
458 values of 2-ΔCT were used to determine the differences, and the data were expressed as the
459 mean ± standard deviation (SD). A significant difference was considered at $P < 0.05$, and
460 extremely significant at $P < 0.01$.
461

462 **Accession Numbers**

463 Sequence data from this article can be found in the Arabidopsis Genome Initiative or
464 GenBank/EMBL data libraries under the following accession numbers: DSP1 (AT4G20060),
465 DSP4 (AT3G07530), CPSF73-I (AT1G61010).
466

467 **Supplemental Data**

468 **Supplemental Figure S1**. Analyses of *dsp4-1*, and the expression pattern of *DSP4*.

469 **Supplemental Figure S2**. Subcellular localization of DSP4.

Supplemental Figure S3. *dsp1-1 dsp4-1* double mutants have complete male sterility.

Supplemental Figure S4. The importance of the DSP4-DSP1 interaction.

Supplemental Figure S5. Pol II occupancy at *Act2* and *Pol II C1* loci.

Supplemental Table S1. Segregation ratio in the offspring of *DSP4/dsp4-1* plants.

Supplemental Table S2. Analysis of gametophyte transmission in heterozygous plants by reciprocal crosses.

Supplemental Table S3. Analysis of gametophyte transmission in double mutants by reciprocal crosses.

Supplemental Table S4. List of primers used in this study.

Acknowledgments

We thank the Tsuyoshi Nakagawa of Shimane University for kindly providing the *pGWBs* vectors. This work was supported by the National Natural Science Foundation of China (31760079), the Project of High Level Innovation Team and Outstanding Scholar in Guangxi Colleges and Universities (2017), the Natural Science Foundation of Guangxi province (2018JJG130001), Innovation Project of Guangxi Education (YCSW2019043), the National Institute of Health (GM127414), and the National Science Foundation (MCB-1808182), Grants from the State Key Laboratory for Conservation and Utilization of Subtropical Agro-bioresources (SKLCUSA-a201919).

Table 1. **Ratio of miscleaved snRNAs in single and double mutants.** The RT-qPCR

products of different snRNA from *dsp1-1 dsp4-1* were cloned into p*MD-18T* vector, and 192 randomly selected clones for each snRNA were sequenced. The miscleaved ratio was calculated as the number of each cleaved type of snRNA clones divided by the total analysis number (192). * NR means Normal Cleaved Ratio of snRNAs, which includes three types of cleavage site (-1 site, middle site and +1 site). # MR means Miscleaved Ratio of snRNAs.

snRNA	Col		*dsp1-1*		*dsp4-1*		*dsp1-1 dsp1-1*	
	NR*	MR #	NR	MR	NR	MR	NR	MR
U1a	28.5: 39.6: 31.9	0	26.7: 40.3: 33.0	0	27.3: 40.3: 32.4	0	21.7: 33.4: 38.6	**6.3**
U2.3	25.2: 40.5: 34.3	0	26.7: 41.7: 31.6	0	27.0: 42.3: 30.7	0	19.6: 35.2: 38.2	**7.0**
U4.2	30.2: 41.2: 28.7	0	29.3: 39.4: 31.3	0	31.6: 38.0: 30.4	0	25.2: 34.8: 33.2	**6.8**
U5-6	20.4: 46.8: 32.8	0	24.3: 47.6: 28.1	0	22.9: 48.4: 28.7	0	19.2: 32.5: 38.8	**9.5**

Figure Legends

Figure 1. *dsp4-1* causes pleiotropic developmental defects.

(A) 25-day-old plants with 9 resette-leaves of Col, *dsp4-1*, and *dsp4-1* harboring the *pDSP4::DSP4-GFP* transgene. (B) Developing seeds in siliques of various genotypes. (C) Alexander staining of pollen grains in anthers of various genotypes. (D) Pollen structures of various genotypes detected by scanning electron microscopy (SEM). (E) *In vitro* germination of pollen of various genotypes. Images were obtained at 8 h after incubation in BK medium. (F) Histochemical GUS staining of pollen (left), embryo sac (middle), and embryos (right) of plants containing the *pDSP4::GUS* transgene. (G) Histochemical staining of GUS in the

siliques of plants containing the *pDSP4::GUS* transgene. DAE: days after emasculation; DAP: days after pollination. (E) and (G) show a representative image of one out of five plants analyzed. Scale bars = 5 mm (A), 1 mm (B), 30 μm (C), 10 μm (D), 20 μm (E), 0.1 mm (F), 0.5 mm (G).

Figure 2. The β-Casp domain of DSP4 and the second ARM cluster of DSP1 mediate the DSP1-DSP4 interaction.

(A) and (B) Schemes of full-length and truncated DSP4 (A) and DSP1 (B) used for testing the DSP1-DSP4 interaction. (C) The interactions of various forms of DSP4 with truncated DSP1 was detected by bimolecular fluorescence complementation (BiFC) in *N. benthamiana* epidermal cells. Paired DSP1-trs-cYFP and DSP4-trs-nYFP fusion proteins were infiltrated into *N. benthamiana* leaves. Green: BiFC signal (originally YFP fluorescence). Red: autofluorescence of chlorophyll. Scale bars=10 μm. (D) Co-immunoprecipitation (Co-IP) of DSP4-tr2 with truncated DSP1 proteins. (E) Co-IP of DSP1-tr2 with truncated DSP4 truncation proteins. IP was performed using antibodies recognizing MYC (D) or GFP (E). After IP, truncated DSP4-MYC and DSP1-GFP were detected by western blot using antibodies against MYC and GFP, respectively. Input: total protein before IP.

Figure 3. Morphological phenotypes of different genotype plants.

(A) and (B) 28-day-old (A) and 48-day-old (B) plants of Col, *dsp1-1*, *dsp4-1*, and *dsp1-1 dsp4-1*. Scale bars = 1.5 cm (A), 3 cm (B). (C) Alexander staining of pollen grains in anthers of Col and *dsp1-1 dsp4-1*. (D) Pollen structures of Col and *dsp1-1 dsp4-1* detected by SEM.

(E) *In vivo* pollen germination of Col and *dsp1-1 dsp4-1*. Images were obtained 8 h after fertilization using *dsp1-1 dsp4-1* (right) or Col as a pollen donor (left). (F) Transmission electron micrographs showing the microspore structures of Col and *dsp1-1 dsp4-1* at anther stage 9. (G) Histochemical GUS staining of inflorescences from *pDSP4::GUS* transgenic plants at different developmental stages. Numbers in the image indicate the developmental stage of flowers. Scale bars = 30 μm (C), 10 μm (D), 0.5 mm (E), 10 μm (F) and 2 mm (G).

Figure 4. DSP1 and DSP4 synergistically promote snRNA 3' end maturation.

(A) and (B) Accumulation of pre-snRNAs (A) and mature snRNA (B) in various genotypes detected by RT-qPCR. The pre-snRNA or mature snRNA levels were normalized to those of *ACT2* and compared with Col (Value set as 1). Values are means of three technical replicates. Bars indicate standard derivation (SD), * $P < 0.05$, ** $P < 0.01$ (t-test). Three biological replicates gave similar results. (C) and (D) Accumulation of pre-*U1a* and -*U2.3* RNAs in various genotypes detected by the RNase protection assay (RPA). Five micrograms of total RNA were incubated with U1a or U2.3 RNA probe. Black arrow indicates pre-snRNAs. Grey arrow indicates mature snRNAs. (E) Abundance of mature *U1* and *U2* snRNAs in various genotypes detected by northern blotting. *Act2* was blotted as the loading control.

Figure 5. DSP1 and DSP4 cooperatively promote pre-snRNA 3' end cleavage.

(A) *In vitro* 3' end processing of *pre-U2.3-polyG* in nuclear protein extracts of various genotypes. *In vitro* transcribed RNAs were labeled at the 5'end and incubated with the nuclear protein. Black arrow indicates the *pre-U2.3-polyG* input. Grey arrow indicates

551 mature snRNA. (B) Histochemical staining of GUS in seedlings (bottom) and inflorescences
552 (top) of Col, *dsp1-1, dsp4-1*, and *dsp1-1 dsp4-1* containing the *pU2::pre-U2-GUS* transgene.
553 Scale bars = 4 mm (top), 1 cm (bottom). (C) *GUS* transcript levels determined by RT-PCR.
554 *Actin* 2 was amplified as a control. (D) *In vitro* GUS activities of protein inflorescence
555 extracts from various genotypes. Protein extracts were quantified and incubated with
556 4-methylumbelliferyl β-D-glucuronide (4-MUG) and the reaction stopped by adding Na_2CO_3
557 after 10 min. The 4-methylumbelliferone (4-MU) products were measured with a
558 spectrophotometer at 595 nm. Values are means of three technical replicates. Bars indicate
559 standard derivation (SD), ** $P < 0.01$ (t-test). (E) 3' end cleavage site of pre-snRNAs in
560 *dsp1-1 dsp4-1*. Green arrows indicate correct cleavage sites. Red arrows indicate improper
561 cleavage sites.
562
563 **Figure 6. DSP1 and DSP4 synergistically promote pre-snRNA transcription.**
564 (A) and (B) Occupancy of Pol II at various sites of the *U1a* (A) and *U2.3* (B) snRNA loci in
565 Col, *dsp1-1*, *dsp4-1*, and *dsp1-1 dsp4-1* detected by chromatin immunoprecipitation. pro:
566 promoter; DS: down-stream region of snRNAs. Values are means of three technical replicates.
567 Bars indicate standard derivation (SD), * $P < 0.05$, ** $P < 0.01$ (t-test). (C) GUS
568 histochemical staining of 28-day-old seedlings (left) and 48-day-old inflorescences (right) in
569 Col, *dsp1-1*, *dsp4-1*, and *dsp1-1 dsp4-1*, containing the *pU2::pre-U2m-GUS* transgene. *m*:
570 mutated 3' box. Scale bars = 4 mm (left), 1cm (right). (D) *GUS* transcript levels determined
571 by RT-PCR. *Actin 2* was amplified as a control. (E) *In vitro* GUS activity in inflorescence
572 protein extracts from various genotypes. The quantified total protein extracts were incubated

573 with 4-MUG, the reaction stopped at 10 min, and 4-MU measured using a spectrophotometer.

574 Values are means of three technical replicates. Bars indicate standard derivation (SD), * P <

575 0.05 (t-test).

576

577

Parsed Citations

Albrecht TR, Shevtsov SP, Wu Y, Mascibroda LG, Peart N, Huang KL, Sawyer IA, Tong L, Dundr M, Wagner EJ (2018) Integrator subunit 4 is a 'Symplekin-like' scaffold that associates with INTS9/11 to form the Integrator cleavage module. Nucleic Acids Res 46: 4241-4255.
Pubmed: Author and Title
Google Scholar: Author Only Title Only Author and Title

Albrecht TR, Wagner EJ (2012) snRNA 3' end formation requires heterodimeric association of integrator subunits. Mol Cell Biol 32: 1112-1123.
Pubmed: Author and Title
Google Scholar: Author Only Title Only Author and Title

Baillat D, Wagner EJ (2015) Integrator: surprisingly diverse functions in gene expression. Trends Biochem Sci 40: 257-264.
Pubmed: Author and Title
Google Scholar: Author Only Title Only Author and Title

Black DL, Chabot B, Steitz JA (1985) U2 as well as U1 small nuclear ribonucleoproteins are involved in premessenger RNA splicing. Cell 42: 737-750.
Pubmed: Author and Title
Google Scholar: Author Only Title Only Author and Title

Carbon P, Murgo S, Ebel JP, Krol A, Tebb G, Mattaj LW (1987) A common octamer motif binding protein is involved in the transcription of U6 snRNA by RNA polymerase III and U2 snRNA by RNA polymerase II. Cell 51: 71.
Pubmed: Author and Title
Google Scholar: Author Only Title Only Author and Title

Carey MF, Peterson CL, Smale ST (2013) The RNase protection assay. Cold Spring Harb Protoc 2013.
Pubmed: Author and Title
Google Scholar: Author Only Title Only Author and Title

Chen J, Wagner EJ (2010) snRNA 3' end formation: the dawn of the Integrator complex. Biochem Soc Trans 38: 1082-1087.
Pubmed: Author and Title
Google Scholar: Author Only Title Only Author and Title

Chen Y, Zou T, McCormick S (2016) S-Adenosylmethionine Synthetase 3 Is Important for Pollen Tube Growth. Plant Physiol 172: 244-53.
Pubmed: Author and Title
Google Scholar: Author Only Title Only Author and Title

Connelly S, Filipowicz W (1993) Activity of chimeric U small nuclear RNA (snRNA)/mRNA genes in transfected protoplasts of Nicotiana plumbaginifolia: U snRNA 3'-end formation and transcription initiation can occur independently in plants. Molecular and cellular biology 13: 6403-6415.
Pubmed: Author and Title
Google Scholar: Author Only Title Only Author and Title

Ezzeddine N, Chen JD., Waltenspiel B, Burch B, Albrecht T, Zhuo M, Warren WD, Marzluff WF., Wagner EJ (2011) A Subset of Drosophila Integrator Proteins Is Essential for Efficient U7 snRNA and Spliceosomal snRNA 3 '-End Formation. Molecular And Cellular Biology 31: 328-341.
Pubmed: Author and Title
Google Scholar: Author Only Title Only Author and Title

Fukudome A, Sun D, Zhang XR, Koiwa H (2017) Salt Stress and CTD PHOSPHATASE-LIKE4 Mediate the Switch between Production of Small Nuclear RNAs and mRNAs. Plant Cell 29: 3214-3233
Pubmed: Author and Title
Google Scholar: Author Only Title Only Author and Title

Gardini A, Baillat D, Cesaroni, M, Hu D, Marinis JM, Wagner EJ, Lazar MA, Shilatifard A, Shiekhattar R (2014) Integrator Regulates Transcriptional Initiation and Pause Release following Activation. Mol Cell 56: 128-39.
Pubmed: Author and Title
Google Scholar: Author Only Title Only Author and Title

Goldberg RB, Beals TP, Sanders PM (1993) Anther development: basic principles and practical applications. Plant Cell 5: 1217-29.
Pubmed: Author and Title
Google Scholar: Author Only Title Only Author and Title

Guiro J, Murphy S (2017) Regulation of expression of human RNA polymerase II-transcribed snRNA genes. Open Biol 7: 170073
Pubmed: Author and Title
Google Scholar: Author Only Title Only Author and Title

Guo ZJ, Karunatilaka KS, Rueda D (2009) Single-molecule analysis of protein-free U2-U6 snRNAs. Nat Struct Mol Biol 16: 1154-U1155.
Pubmed: Author and Title
Google Scholar: Author Only Title Only Author and Title

Hadjiolov AA, Venkov PV, Tsanev RG (1966) Ribonucleic acids fractionation by density-gradient centrifugation and by agar gel electrophoresis: a comparison. Analytical biochemistry 17: 263-267.

Pubmed: Author and Title
Google Scholar: Author Only Title Only Author and Title

Hata T, Nakayama M (2007) Targeted disruption of the murine large nuclear KIAA1440/Ints1 protein causes growth arrest in early blastocyst stage embryos and eventual apoptotic cell death. Biochim Biophys Acta 1773: 1039-51.
Pubmed: Author and Title
Google Scholar: Author Only Title Only Author and Title

Jodoin JN, Shboul M, Albrecht TR, Lee E, Wagner EJ, Reversade B, Lee LA (2013) The snRNA-processing complex, Integrator, is required for ciliogenesis and dynein recruitment to the nuclear envelope via distinct mechanisms. Biology Open 2: 1390-1396.
Pubmed: Author and Title
Google Scholar: Author Only Title Only Author and Title

Kapp LD, Abrams EW, Marlow FL, Mullins MC (2013) The integrator complex subunit 6 (Ints6) confines the dorsal organizer in vertebrate embryogenesis. PLoS Genet 9: e1003822.
Pubmed: Author and Title
Google Scholar: Author Only Title Only Author and Title

Koizumi K, Wu S, MacRae-Crerar A, Gallagher KL (2011) An essential protein that interacts with endosomes and promotes movement of the SHORT-ROOT transcription factor. Curr Biol 21: 1559-64.
Pubmed: Author and Title
Google Scholar: Author Only Title Only Author and Title

Kolev NG, Yario TA. Benson E, Steitz JA (2008) Conserved motifs in both CPSF73 and CPSF100 are required to assemble the active endonuclease for histone mRNA 3'-end maturation. EMBO Rep 9: 1013-8
Pubmed: Author and Title
Google Scholar: Author Only Title Only Author and Title

Lai F, Gardini A, Zhang A, Shiekhattar R (2015) Integrator mediates the biogenesis of enhancer RNAs. Nature 525: 399-403.
Pubmed: Author and Title
Google Scholar: Author Only Title Only Author and Title

Li YF, Si LL, Zhai Y, Hu YL, Hu ZB, Bei JX, Xie BB, Ren Q, Cao PB, Yang F, Song QF, Bao ZY, Zhang HT, Han YQ, Wang ZF, Chen X, Xia X, Yan HB, Wang R, Zhang Y, Gao CM, Meng JF, Tu XY, Liang XQ, Cui Y, Liu Y, Wu XP, Li Z, Wang HF, Li ZX, Hu B, He MH, Gao ZB, Xu XB, Ji HZ, Yu CH, Sun Y, Xing BC, Yang XB, Zhang HY, Tan AH, Wu CL, Jia WH, Li SP, Zeng YX, Shen HB, He FC, Mo ZN, Zhang HX, Zhou GQ (2016) Genome-wide association study identifies 8p21.3 associated with persistent hepatitis B virus infection among Chinese. Nature Communications 7: 11664.
Pubmed: Author and Title
Google Scholar: Author Only Title Only Author and Title

Liu Y, Li S, Chen Y, Kimberlin AN, Cahoon EB, Yu B (2016) snRNA 3′ End Processing by a CPSF73-Containing Complex Essential for Development in Arabidopsis. Plos Biology 14: e1002571.
Pubmed: Author and Title
Google Scholar: Author Only Title Only Author and Title

Nakagawa T, Kurose T, Hino T, Tanaka K, Kawamukai M, Niwa Y, Toyooka K, Matsuoka K, Jinbo T, Kimura T (2007) Development of series of gateway binary vectors, pGWBs, for realizing efficient construction of fusion genes for plant transformation. J Biosci Bioeng 104: 34-41.
Pubmed: Author and Title
Google Scholar: Author Only Title Only Author and Title

Ohtani M, Demura T, Sugiyama M (2008) Differential requirement for the function of SRD2, an snRNA transcription activator, in various stages of plant development. Plant Molecular Biology 66: 303-314.
Pubmed: Author and Title
Google Scholar: Author Only Title Only Author and Title

Ray R, Ray K, Panda CK (1997) Differential alterations in metabolic pattern of the six major UsnRNAs during development. Molecular And Cellular Biochemistry 177: 79-88.
Pubmed: Author and Title
Google Scholar: Author Only Title Only Author and Title

Rutkowski RJ, Warren WD (2009) Phenotypic analysis of deflated/Ints7 function in Drosophila development. Dev Dyn 238: 1131-9.
Pubmed: Author and Title
Google Scholar: Author Only Title Only Author and Title

Sanders PM, Bui AQ, Weterings K, McIntire KN, Hsu YC, Lee PY, Truong MT, Beals TP, Goldberg RB (1999) Anther developmental defects in Arabidopsis thaliana male-sterile mutants. Sexual Plant Reproduction 11: 297-322.
Pubmed: Author and Title
Google Scholar: Author Only Title Only Author and Title

Skaar JR, Ferris AL, Wu X, Saraf A, Khanna KK, Florens L, Washburn MP, Hughes SH Pagano M (2015) The Integrator complex controls the termination of transcription at diverse classes of gene targets. Cell Research 25: 288-305.
Pubmed: Author and Title
Google Scholar: Author Only Title Only Author and Title

Stadelmayer B, Micas G, Gamot A, Martin P, Malirat N, Koval S, Raffel R, Sobhian B, Severac D, Rialle S (2014) Integrator complex regulates NELF-mediated RNA polymerase II pause/release and processivity at coding genes. Nature Communications 5: 5531.
Pubmed: Author and Title
Google Scholar: Author Only Title Only Author and Title

Sullivan KD, Steiniger M, Marzluff WF (2009) A core complex of CPSF73, CPSF100, and Symplekin may form two different cleavage factors for processing of poly(A) and histone mRNAs. Mol Cell 34: 322-32
Pubmed: Author and Title
Google Scholar: Author Only Title Only Author and Title

Tao S, Cai Y, Sampath K (2009) The Integrator subunits function in hematopoiesis by modulating Smad/BMP signaling. Development 136: 2757-65.
Pubmed: Author and Title
Google Scholar: Author Only Title Only Author and Title

Uguen P, Murphy S (2003) The 3' ends of human pre-snRNAs are produced by RNA polymerase II CTD-dependent RNA processing. EMBO J 22: 4544-54.
Pubmed: Author and Title
Google Scholar: Author Only Title Only Author and Title

Uguen P, Murphy S (2004) 3 '-Box-dependent processing of human pre-U1 snRNA requires a combination of RNA and protein co-factors. Nucleic Acids Research 32: 2987-2994.
Pubmed: Author and Title
Google Scholar: Author Only Title Only Author and Title

Vankan P, Filipowicz W (1988) Structure of U2 snRNA genes of Arabidopsis thaliana and their expression in electroporated plant protoplasts. The EMBO journal 7: 791.
Pubmed: Author and Title
Google Scholar: Author Only Title Only Author and Title

Wu Y, Albrecht TR, Baillat D, Wagner EJ, Tong L (2017) Molecular basis for the interaction between Integrator subunits IntS9 and IntS11 and its functional importance. Proc Natl Acad Sci USA 114: 4394-4399
Pubmed: Author and Title
Google Scholar: Author Only Title Only Author and Title

Wang B, Xue JS, Yu YH, Liu SQ, Zhang JX, Yao XZ, Liu ZX, Xu XF, Yang ZN (2017) Fine regulation of ARF17 for anther development and pollen formation. BMC Plant Biol 17: 243
Pubmed: Author and Title
Google Scholar: Author Only Title Only Author and Title

Xie MY, Zhang W, Shu, MD, Xu A, Lenis DA, DiMaio D, Steitz JA (2015) The host Integrator complex acts in transcription-independent maturation of herpesvirus microRNA 3 ' ends. Genes & Development 29: 1552-1564.
Pubmed: Author and Title
Google Scholar: Author Only Title Only Author and Title

Xu XF, Wang B, Lou Y, Han WJ, Lu JY, Li DD, Li LG, Zhu J, Yang ZN (2015) Magnesium Transporter 5 plays an important role in Mg transport for male gametophyte development in Arabidopsis. Plant Journal 84: 925-936.
Pubmed: Author and Title
Google Scholar: Author Only Title Only Author and Title

Xu R, Zhao H, Dinkins RD, Cheng X, Carberry G, Li QQ (2006) The 73 kD subunit of the cleavage and polyadenylation specificity factor (CPSF) complex affects reproductive development in Arabidopsis. Plant Mol Biol 61: 799-815.
Pubmed: Author and Title
Google Scholar: Author Only Title Only Author and Title

Zhang S, Xie M, Ren G, Yu B (2013) CDC5, a DNA binding protein, positively regulates posttranscriptional processing and/or transcription of primary microRNA transcripts. Proc Natl Acad Sci USA 110: 17588-17593.
Pubmed: Author and Title
Google Scholar: Author Only Title Only Author and Title